



Acoustic Scintillation Flow Measurements in the Intake at Kootenay Canal Power Plant

David D. Lemon and David Billenness

ASL AQFlow Inc.
Sidney, BC, Canada

See also ASME Performance Test Code Committee paper (click on paper title below):

[Results of Kootenay canal flow comparison test using intake methods \(Hydro 2010\)](#)

Introduction

Acoustic Scintillation was one of the three intake flow measurement methods tested in the comparisons carried out in Unit #1 at BC Hydro's Kootenay Canal power plant in October, 2009, sponsored by CEATI (the Centre for Energy Advancement through Technological Innovation) and supervised by the PTC-18 Committee of the ASME. The comparison was run as a blind test; none of the test participants had knowledge of the reference or any other test discharges until after the final results were submitted 30 days after the completion of the measurements.

Each unit at Kootenay Canal has a single intake, 7.44 m high and 4.88 m wide. Both current meters and acoustic scintillation sensors had to be deployed in the maintenance gate slot, the only one available for installing instruments. The preferred method to install Acoustic Scintillation Flow Meter (ASFM) sensors is on a fixed frame deployed in a slot. In this case, the slot was wide enough that a combined frame could be used, thus allowing both systems to be operated at the same time, which greatly reduced the time required to collect data and meant that comparisons among all the test and reference methods could be made with simultaneous data. The current meters were mounted on the cross-member of a travelling frame, or trolley, which moved up and down within the larger stationary frame. The ASFM arrays were mounted in pairs on opposite vertical sides of the stationary part of the frame, upstream of the current meter frame.

The ASFM transducer pairs formed sixteen sampling paths, spaced at 0.46m vertically. Two paths could be sampled simultaneously: one from the upper 8 and one from the lower 8. The sampling order for the paths had to be arranged such that any two active paths were never within 0.5m of each other or the position of the current meter frame.

Each ASFM acoustic path was sampled for 50 seconds; a discharge measurement therefore required approximately 8 minutes, and three could be made at each condition while the current meter sampling was under way. The procedures used to compute the laterally-averaged velocity at each path, and their integration to compute the discharge (including estimation of the boundary layer contribution) are described. The mean of the three individual discharges was reported as the result for each of the 36 flow conditions in the primary program. The results were reported immediately following each run at the site; a period of 30 days was then allowed for review and checking. The final results differed from the field results by an average of 0.04%.

The mean difference between the ASFM discharges and the reference was 0.44%.

1. ASFM Measurement Principle

The ASFM uses a technique called acoustic scintillation drift (Clifford & Farmer, 1983; Farmer & Clifford, 1986) to measure the flow velocity perpendicular to a number of acoustic paths established across the intake to the turbine. Short (16 μ sec) pulses of high-frequency sound (307 kHz) are sent from transmitting arrays on one side to receiving arrays on the other, at a rate of approximately 250 pings /second. Fluctuations in the amplitude of those acoustic pulses result from turbulence in the water carried along by the current. The ASFM measures those fluctuations (known as scintillations) and from them computes the lateral average (i.e. along the acoustic path) of the velocity perpendicular to each path.

The ASFM utilizes the natural turbulence embedded in the flow, as shown in Fig. 1. In its simplest form, two transmitters are placed on one side of the measurement section, two receivers at the other. The signal amplitude at the receivers varies randomly as the turbulence along the propagation paths changes with time and the flow. If the two paths are sufficiently close (Δx), the turbulence remains embedded in the flow, and the pattern of these amplitude variations at the downstream receiver will be nearly identical to that at the upstream receiver, except for a time delay, Δt . This time delay corresponds to the peak in the time-lagged cross-correlation function calculated for Signal 1 and Signal 2. The mean velocity perpendicular to the acoustic paths is then $\Delta x / \Delta t$. Using three transmitters and three receivers at each measurement level allows both the magnitude and

inclination of the velocity to be measured. The ASFM computes the discharge through each bay of the intake by integrating the horizontal component of the velocity over the cross-sectional area of the intake. In a multi-bay intake, the discharges through each bay are summed to compute the total discharge.

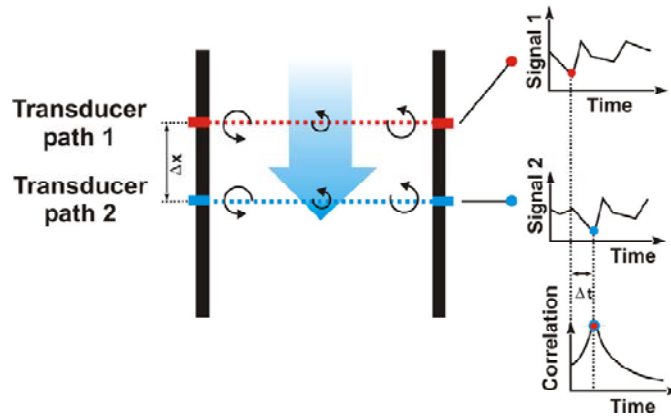


Fig. 1: Schematic representation of acoustic scintillation drift.

2. ASFM Implementation at Kootenay Canal

The ASFM sensors were installed in the maintenance gate slot, as indicated in Figure 2; the current meters were also to be deployed in the same slot. To save the time that would have been required to remove the equipment for one method, replace it with the other and then repeat test sequences, the support frame for the ASFM transducers was designed to include a channel for the moving trolley that carried the current meters. This allowed an entire program to be completed in the time the plant was available. Figure 3 shows a schematic drawing of the support frame used at Kootenay Canal.

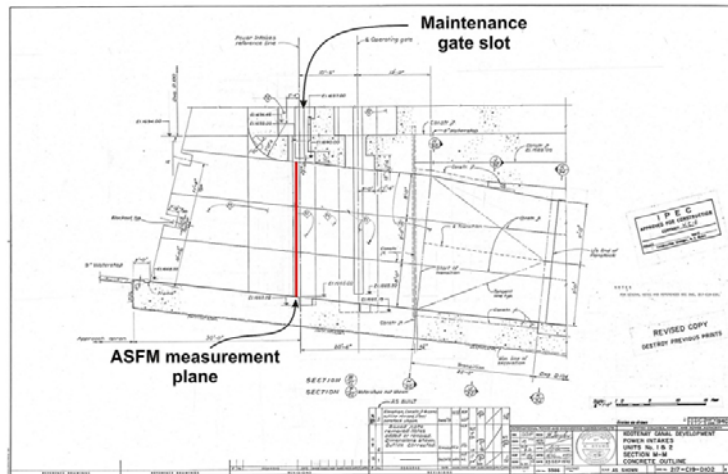


Fig. 2: Location of the ASFM sensor plane in Unit 1 intake.

The intake was small enough that the frame could be built without a bottom cross-bar, with the box members on the side and the double top cross-bars providing sufficient stiffness to maintain the position of the side members. The side faces were designed to sit flush with the intake walls once the frame was lowered into place. BC Hydro designed the frame in consultation with ASL and Hydro-Quebec, and contracted for its construction.

The rows of holes for the ASFM transducers were placed close to the upstream edge of the frame side faces. The transducers were placed with their faces flush with the sides of the frame so that the full width of the intake was sampled and the transducers were protected from debris.

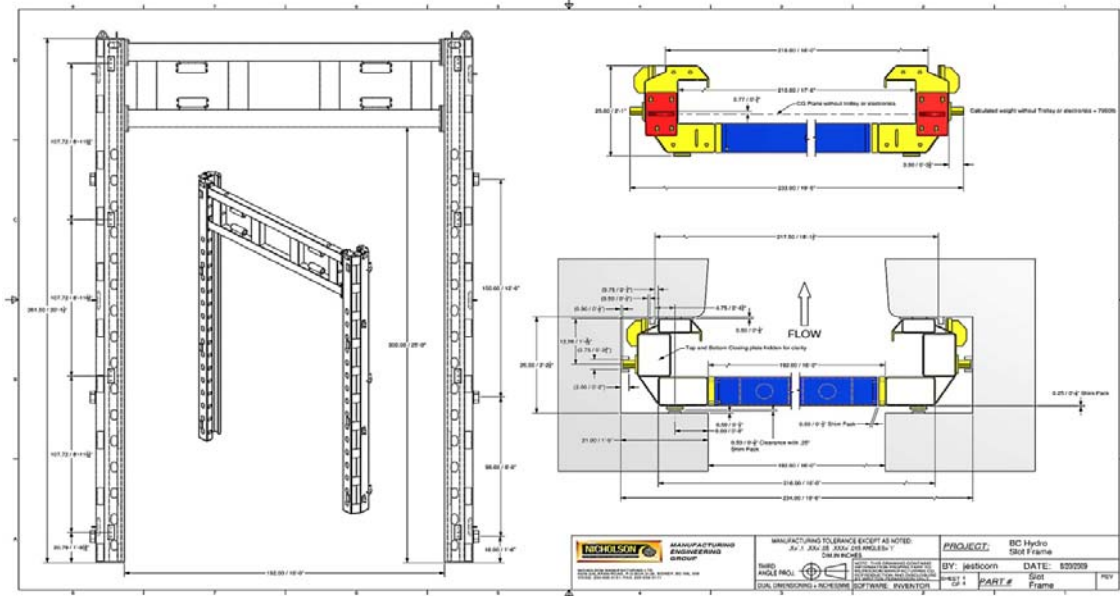


Fig. 3: Schematic of the frame.

Sixteen pairs of holes for the arrays were provided on the frame, with the lowest pair 30 cm above the bottom of the frame, and the uppermost pair 30 cm below the roof elevation. The remaining 14 pairs of holes were spaced equally between the uppermost and lowest pairs, resulting in sampling paths spacing of 45.6 cm in the vertical.

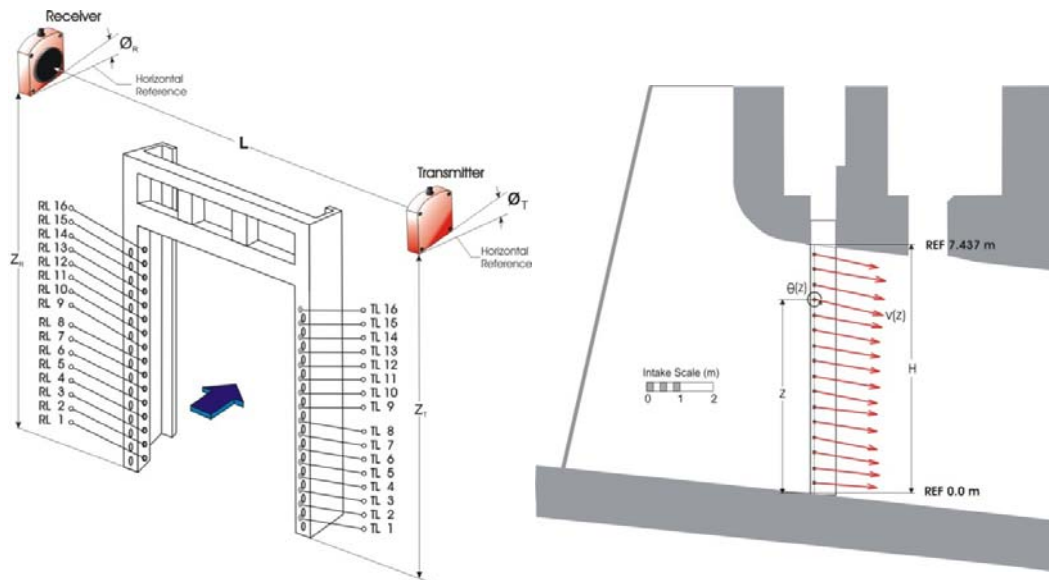


Figure 4: Schematic diagram of the sensor layout and definition of geometrical parameters.

Figure 4 shows the arrangement of the transducers on the frame schematically in the left panel, and defines the additional geometric parameters used in the discharge calculation in the right panel. Those parameters were measured before and after the test; the pre-deployment values were used to compute the field discharges, while the average of the two sets was used in the final calculations. At Kootenay Canal, the intake has only one bay and the ASFM was configured with two 8-path groups; one in the upper half of the intake, the other in the lower. The surface equipment was housed in a trailer on the intake deck. Figures 5 and 6 show the equipment on the frame and the deployment of the frame into the maintenance gate slot.

3. Operational Checks

The frame was deployed into the maintenance gate slot on October 19th, and preliminary operational checks with no flow present were successfully completed. On October 20th, the coordinated sampling scheme for the ASFM



Figure 5: A view of the ASFM equipment mounted on the frame.



Figure 6: Transducer support frame being deployed into the gate slot.

and the current meters was tested with no flow present, and adjusted until both technologies could operate simultaneously without interference. The unit was re-watered in the late afternoon, and further operational checks at speed-no-load flow were performed. The data quality was good and no interference was observed from the current meters nor was there any interference between the ASFM and the acoustic time-of-travel instrument installed further downstream in the intake. In the final coordinated sampling scheme, at each test point, one pass of the current meter trolley through 20 fixed elevations was made, requiring 20 minutes to complete. While the trolley was in motion, the ASFM went through two sampling runs. During each run, two paths, one in the upper group and one in the lower group, were sampled simultaneously for 50 seconds each; each run required approximately 8 minutes. The order in which the paths were sampled was selected so that the two active acoustic paths were never within less than 0.5 metre of each other or the current meters. Four different sampling orders were used, corresponding to upward or downward passes of the current meter trolley, and whether the trolley was in the first or second half of its pass. A third ASFM run, using 33-second sampling at each level (4.5 minutes duration) was added at the end of each pass of the current meter trolley, since there was usually time available, especially on upward passes, where the trolley moved up above the roof level. Two additional sampling orders were used for these final ASFM runs.

On October 21st, the unit was operated at mid-range flows to allow further operational checks by all the flow measurement groups at higher velocities. No interference from the current meters was observed, and there was no evidence of any vibration from the frame or trolley in the ASFM data.

4. Data Collection

The test program began at noon October 21st. To minimize head variations in the canal, the total discharge through the power plant was maintained as nearly constant as possible during the tests. In the primary test program, the balancing flow was always provided by the same unit (#3). A secondary test program was also carried out in which the unit providing balance flow alternated between units #2 and #3. The 36 conditions in the primary test program were completed on October 23rd. Three ASFM runs were made at each test point (coordinated with the current meter trolley movements described earlier), and the reported discharge was the average of the three runs. The 10 runs in the secondary program were completed on October 24th. Some additional tests of an alternate method for mounting the ASFM (a single path mounted on the travelling current meter frame) were also done after the primary program, but will not be dealt with in this paper.

5. Data Analysis and Results

Preliminary values for the velocity and discharge were produced immediately after each run. The discharge was computed as the average of the discharges from each of the three individual runs made at each test point, integrated using a quadratic interpolation scheme in the profile of the horizontal component of velocity.

5.1 Velocities

The basis of the ASFM velocity measurement is the time-lagged correlation of the time series of acoustic amplitude fluctuations recorded over two spatially separated paths. Three time series were collected at each level during the normal course of these tests; each sequence was treated as follows: The amplitude fluctuations are random variables, and the time delay between them as measured by the position of the peak of the time-lagged cross-correlation is a statistical quantity. A measure of its variability is derived by subdividing the full length of the time series (50 seconds at 250 Hz pinging rate) into N segments of 2048 samples (six 2048 point blocks, each 8.2 seconds long at 250 Hz pinging rate). The individual blocks are 2048 points long for computational efficiency in the Fast Fourier Transform procedure used to compute the cross-correlation.

Before computing the cross-correlations and the velocity, the acoustic amplitude data were band-pass filtered. The passband frequency limits were selected from one of three sets, designed to maintain the same wavenumber range in the turbulence as the source of the amplitude fluctuations. An initial estimate of the flow velocity (computed from data filtered with a fixed passband of 6.5 to 40 Hz) was used to select the passband limit set; the upper limit of each set was fixed, and the lower limit was selected from a range of frequencies specific to each set. The selection was an iterative process; the lower limit frequency, f_L , was incremented in 1 Hz steps from the minimum to the maximum of the range for the first few blocks of data. The peak cross correlation values for the three pairs of time series for each block were recorded, and those above a threshold value of 0.2 (the theoretical minimum) were retained. A quality index, QI, was then computed as the product of the ratio of the average peak correlation score for each pair to the theoretical maximum and the fraction of the scores that were retained as being above the threshold value. The procedure was repeated for each value of f_L , and the value with the highest QI was used to filter the entire data set. The three peak cross-correlations and time delays for each block were then computed. The velocity was computed from their averages, after rejection of outliers. Outliers were rejected using the Grubbs T-statistic (International Electrotechnical Commission, 1991). For example, in a 6 block set, values more than 1.89 standard deviations from the mean were removed. The quality index QI was recomputed after outlier rejection.

The laterally-averaged values of the velocity magnitude and inclination for each path were calculated at each level from the individual replicate runs. The discharge was calculated from the average of the individual replicate discharges and not from the integration of the average velocity (i.e. the discharge was calculated from each of the individual runs and then averaged instead of averaging the velocities and then calculating a discharge). This method gave independent discharge samples which were used to compute a standard deviation from the individual runs.

The data computed from each of the replicates was plotted and examined manually; there were only two velocity values that were removed in the entire set of data. The first was from test P1 in the third replicate run, where the current meters arrived at the bottom more quickly than anticipated and interfered with the acoustic signal. The sampling procedure was modified after that, and the problem did not recur. The second instance occurred when evidence was found of several disturbances passing through the acoustic beam on one of the paths and distorting the correlation curves.

Figure 7 shows a sample of the velocity vector plots. The base of each vector is located at the position in the intake where the measurement was made. The length of the vector gives the magnitude of the velocity, scaled by the legend in the diagram, and its direction shows the inclination. The number at the base of each vector is its magnitude in metres per second. The notations at the top of the figure detail the conditions under which the data were collected. The heavy arrows are the average of the individual velocities from each replicate run, which are shown as the lighter arrows (mostly obscured by the average).

5.2 Velocity Uncertainty

The relative uncertainty is a measure of the random uncertainty in the horizontal component of the velocity computed from each of the three repeat runs. The relative uncertainty for each individual run is computed as:

$$\Delta v = \frac{\sigma}{\tau_{av}} \quad (5-1)$$

where τ_{av} is the average time delay over the N blocks for the pair of elements with the highest peak cross-

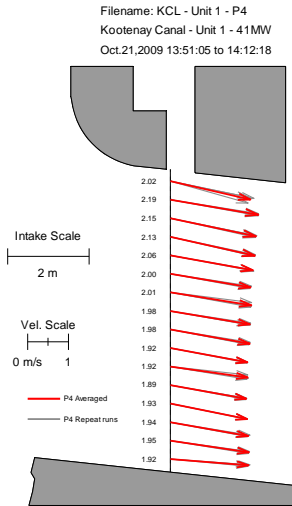


Figure 7: Sample velocity vector plot.

correlation score (they are the most closely aligned with the flow direction) and σ is its standard deviation. The random error is further reduced by averaging the replicate runs together. The average relative uncertainty at each level is calculated from three runs as:

$$\overline{\Delta v} = \frac{\sqrt{(\Delta v_1 \cdot V_{h_1})^2 + (\Delta v_2 \cdot V_{h_2})^2 + (\Delta v_3 \cdot V_{h_3})^2}}{\overline{V}_h} \quad (5-2)$$

where Δv_1 , Δv_2 , and Δv_3 are the individual relative uncertainties from three runs, V_{h_1} , V_{h_2} , and V_{h_3} are the horizontal velocities of the three runs, and \overline{V}_h is the average horizontal velocity computed from the replicate runs.

5.3 Discharge Computation

The roof and floor of the intake and the sides of the frame holding the ASFM transducers define a plane surface, S, through which the flow must pass. The discharge is therefore given by the flux through S:

$$Q = \oint_S \mathbf{V} \cdot \mathbf{n} \, da \quad (5-3)$$

where \mathbf{V} is the velocity vector (a function of position in the plane) and \mathbf{n} is the unit vector normal to the plane. The ASFM measures the lateral average of the component of velocity normal to the propagation path; if z' is the vertical coordinate, then the discharge, Q , in terms of the laterally-averaged velocity, v , is:

$$(5-4)$$

where $v(z')$ is the magnitude of the laterally-averaged velocity at elevation z' , $\theta(z')$ is the corresponding inclination angle, $L(z')$ is the width between the transducer faces, and H is the height of the intake roof above the floor. The lateral averaging performed by the ASFM is continuous, while the sampling in the vertical was at sixteen discrete points. Calculating Q then required estimation of the integral in equation 5-4 when the integrand was known at a finite number of points. The integral was evaluated numerically using a Romberg integration, with a quadratic interpolation in the integrand between the measured points. The accuracy of the integration depends on the sampling levels being placed properly to resolve the variation of the horizontal velocity with elevation; 16 paths were used in this case to ensure that any such variations were fully resolved. The measured points do not extend all the way to the intake roof and floor; as a result, complete evaluation of the integral required an evaluation of the flow in the zones next to those boundaries.

It was necessary to assume a form for the normal component of the velocity to allow the evaluation of the integral to be completed between the measured points at the top and bottom extremes and the corresponding boundaries at the roof and floor. A closed boundary was imposed in both cases. At the floor, a curve of the form:

$$\left[\frac{z}{T} \right]^X \quad (5-5)$$

was fitted for the measured profiles in between the floor ($z = 0$) and the boundary thickness T . During the measurements at the site, T was set to 0.30 m, the elevation of the lowest measurement path, and X was set to 7.

At the roof, a curve of the form:

$$\left[\frac{Z_r - z}{T} \right]^X \quad (5-6)$$

was fitted with the same initial choices of the parameters T and X .

The assumptions made for the boundary layers were reviewed after the conclusion of the field program, with the assistance of the measured profiles of the horizontal velocity component. Two of the positions measured with the single array pair on the moving trolley were between the uppermost level (#16) on the fixed frame and the roof. When plotted together with the upper boundary form of Equation 5-6, it was apparent that setting $X = 7$ overestimated V_h at those elevations. Setting the parameter X to 4 instead of 7 produced a better fit. T was left unchanged.

In the lower boundary layer, the profiles of V_h do not show any consistent indication of decrease at 0.30 m elevation, which suggests that the boundary layer thickness, T , used in the field was too large. A review of the theoretical development of boundary layers for an accelerating flow over a flat plate was made for conditions approximating those in the Kootenay Canal intake. The conclusion drawn was that the lower boundary layer would be more realistically represented with a thickness, T , of 0.125 m and the X parameter set to 9, representative of a nearly smooth surface. The total discharge is relatively insensitive to changes in the form of the lower boundary layer; varying the displacement thickness over the likely range of surface roughness for the full range of flow values produced a maximum change in the discharge of 0.25%.

The final discharge values were then recalculated using the modified upper and lower boundary conditions and incorporating the minor adjustments arising from the post-deployment frame dimension measurements. The result was a small increase over the discharges computed in the field, arising almost entirely from the boundary adjustments: the average increase was 0.04%; the maximum was 0.11% and the minimum was 0.

5.4 Discharge Results

The final discharge values are listed in Table 1, in chronological order. It lists the discharge from each of the

Test Point	Q (m ³ /s)	σ/Q _{avg}	Test Point	Q (m ³ /s)	σ/Q _{avg}	Test Point	Q (m ³ /s)	σ/Q _{avg}
P1	70.73	0.23%	P17	106.26	0.12%	P33	37.81	0.35%
P2	70.57	0.16%	P18	106.25	0.19%	P34	37.88	0.61%
P3	70.66	0.38%	P19	106.21	0.38%	P35	37.64	0.52%
P4	70.75	0.20%	P20	106.24	0.14%	P36	37.78	0.28%
P5	106.10	0.06%	P21	105.94	0.26%	Secondary Test Program		
P6	106.30	0.36%	P22	106.25	0.30%	S1	37.94	0.22%
P7	106.11	0.09%	P23	106.15	0.30%	S2A	38.35	0.18%
P8	106.25	0.30%	P24	106.09	0.07%	S2B	38.24	0.25%
P9	37.98	0.02%	P25	37.85	0.58%	S5A	70.98	0.31%
P10	37.99	0.43%	P26	37.90	0.07%	S5B	70.94	0.45%
P11	37.94	0.23%	P27	37.74	0.21%	S9A	106.28	0.43%
P12	38.07	0.27%	P28	37.82	0.45%	S9B	106.23	0.13%
P13	70.81	0.26%	P29	70.60	0.29%	S10	106.26	0.26%
P14	70.92	0.13%	P30	70.87	0.18%	S6	70.74	0.27%
P15	70.76	0.53%	P31	70.51	0.05%	S8	70.70	0.52%
P16	70.80	0.20%	P32	70.60	0.23%			

Table 1: Final discharge values (in chronological order).

replicate runs used to compute the average discharge at each test point and the corresponding fractional standard deviation. Sample plots of the horizontal component of the velocity for each nominal discharge are given in Figure 8. The red line is a quadratic interpolation of the average V_h ; the black lines are the quadratic interpolation through the measurements from each repeat run; the blue line is an extrapolation from the last measurement point to the floor/roof thickness T ; the dotted line is the curve calculated from equations (5-5) and (5-6), with the revised values for T and X .

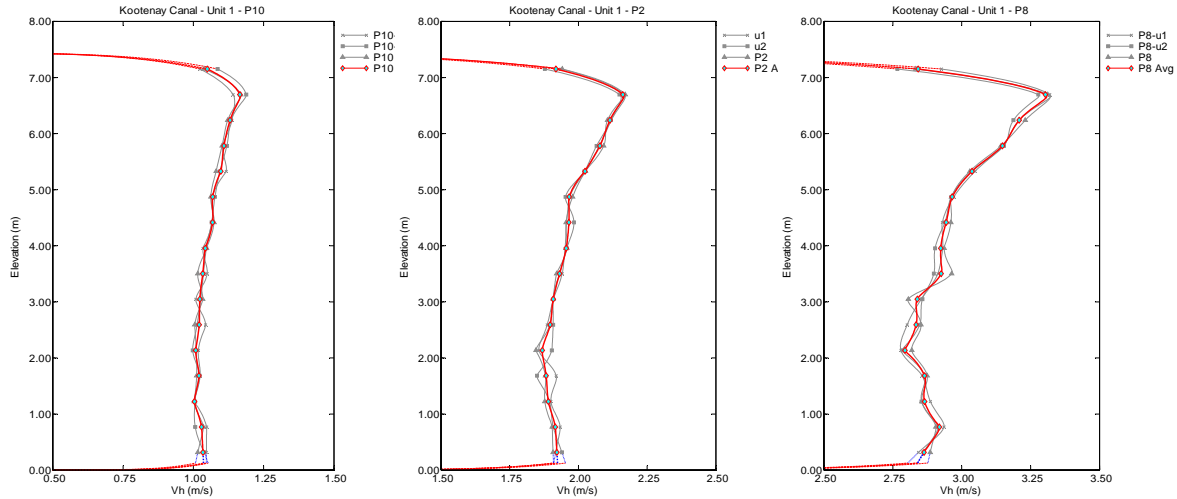


Figure 8: Sample plots of the horizontal component of velocity for low, medium and high flow.

5.5 Discharge Uncertainties

The replicate runs made at each condition allowed an estimate of the random error in the ASFM flow measurements to be calculated. Table 1 lists the mean discharge and the standard deviation of the replicate runs divided by the average discharge (σ/Q_{avg}) as a percentage. The average fractional standard deviation of the discharge at each test point is 0.27% and the maximum is 0.61%.

Since each of the primary program test conditions was repeated 12 times, a preliminary evaluation of the repeatability of the ASFM discharge measurement could be made. The flow values in Table 1 have not been adjusted for any variations in head, but as conditions were kept as nearly constant as possible during the tests to minimize variability, the preliminary repeatability figures are likely to be an upper bound. The standard deviations of the ASFM flows in the primary program were 0.32% at the low flow condition, 0.18% at the medium flow condition and 0.10% at the high flow condition. In absolute terms, these variations correspond to 0.12, 0.13 and 0.10 m^3/sec at the low, medium and high flow conditions, nearly a constant value. These standard deviations are close to those found for the other intake methods and the reference measurement in the penstock.

6. Conclusions and Comparison with Reference Flow

The quality of the data collected by the ASFM throughout the test programs was good, as measured by the instrument's internal criteria. Out of the entire data set, only two path velocities were rejected (out of 2208 in total), one of which was due to interference from the current meter trolley. The final discharge results, after re-evaluating the boundary layer forms and including the post-deployment frame measurements, were slightly higher than the field values: on average by 0.04%, with the greatest difference being 0.11%.

Agreement with the reference flow was very good in both the primary and secondary test programs. In the primary test program, the average deviation of the ASFM flow from the reference flow was 0.44%, with a standard deviation of 0.19%. The difference showed no significant trend with discharge.

In the secondary test program, the average deviation from the reference flow was 0.61%, with a standard deviation of 0.41%. There was no significant correlation between the deviations and the unit used for balancing flow. Given the smaller number of samples in the secondary program (10 vs. 36 for the primary program), the agreement is effectively the same.

References

Clifford, S.F. and D.M. Farmer, 1983. Ocean flow measurements using acoustic scintillation. J. Acoust. Soc. Amer., 74 (6). 1826-1832.

Farmer, D.M. and S.F. Clifford, 1986. Space-time acoustic scintillation analysis: a new technique for probing ocean flows. IEEE J. Ocean. Eng. OE-1 1(1), 42 - 50.

International Electrotechnical Commission, 1991. Field acceptance tests to determine the hydraulic performance of hydraulic turbines, storage pumps and pump-turbines, IEC International Standard 600041.

Acknowledgements

The authors wish to thank the staff at Kootenay Canal Generating Station as well as the BC Hydro test personnel for their cooperation and assistance during the installation and operation of the ASFM. ASL's participation in the test was partially funded through CEATI International Inc. Agreement No. T092700-0358C.

The Authors

David Lemon, M.Sc., graduated in Physics (Oceanography) from the University of British Columbia, Vancouver, in 1975. He is President of ASL AQFlow Inc., Victoria, B.C., with responsibility for internal research and development. He has been responsible for the development of the acoustic scintillation method.

David Billenness, M.A.Sc., graduated from the University of Victoria, British Columbia, in 1995 and has worked for ASL Environmental Sciences since 1997. He currently heads the field flow measurement program associated with the ASFM.